Simulations of the time and space-resolved x-ray transmission of a free-electron-laser-heated aluminium plasma

2016 J. Phys. B: At. Mol. Opt. Phys. 49 035603

(http://iopscience.iop.org/0953-4075/49/3/035603)

OPEN ACCESS
IOP Publishing
Journal of Physics B: Atomic, Molecular and Optical Physics
J. Phys. B: At. Mol. Opt. Phys. **49** (2016) 035603 (7pp)
doi:10.1088/0953-4075/49/3/035603

Simulations of the time and space-resolved x-ray transmission of a free-electron-laser-heated aluminium plasma

D S Rackstraw[1], S M Vinko[1], O Ciricosta[1], H-K Chung[2], R W Lee[3] and J S Wark[1]

[1] Department of Physics, Clarendon Laboratory, University of Oxford, Parks Road, Oxford OX1 3PU, UK
[2] Atomic and Molecular Data Unit, Nuclear Data Section, IAEA, PO Box 100, A-1400 Vienna, Austria
[3] Department of Physics, University of California, Berkeley, CA 94720, USA

E-mail: justin.wark@physics.ox.ac.uk

Received 13 October 2015, revised 12 November 2015
Accepted for publication 23 November 2015
Published 21 January 2016

Abstract

We present simulations of the time and space-resolved transmission of a solid-density aluminium plasma as it is created and probed with the focussed output of an x-ray free-electron-laser with photon energies ranging from the *K*-edge of the cold material (1560 eV) to 1880 eV. We demonstrate how information about the temporal evolution of the charge states within the system can be extracted from the spatially resolved, yet time-integrated transmission images. We propose that such time-resolved measurements could in principle be performed with recently developed split-and-delay techniques.

Keywords: free-electron laser, x-ray, transmission

(Some figures may appear in colour only in the online journal)

1. Introduction

The high intensities and short pulse lengths afforded by x-ray free-electron-lasers (FELs) such as the linear coherent light source (LCLS) allow for the generation and diagnosis of plasmas at exactly solid density [1]. The *K*-shell emission from these solid density plasmas has led to new measurements of continuum lowering [2], as well as the study of resonant interactions between the laser and the $K-L$ transitions in the various ion stages present within the plasma as it heats up and evolves [3, 4]. As well as emission measurements, a study of the transmission of the FEL beam has demonstrated saturable absorption: as the system is heated and ionised during the pulse the energy of the *K*-edge of ions of increasing charge themselves increase, and can exceed that of the energy of the incident FEL photons, leading to increased transmission [5].

The time-integrated emission spectra and transmission data from the experiments discussed above are well-modelled by the collisional-radiative code SCFLY [6] which has been adapted to simulate x-ray FEL interactions with matter, and bench-marked against the first atomic kinetics experiments performed at LCLS [7]. While the experimental data is integrated in time over the FEL pulse (which for the work cited above is typically of order 100 fsec FWHM), the code simulates the full temporal history of the charge states and populations of the superconfigurations, as well as providing temporally resolved x-ray spectra and transmission data.

In this context it is thus of interest to consider how one might obtain experimentally temporally resolved information about the charge state evolution to compare with simulations, thus providing more detailed information about the evolution of the system. We posit that such a time-resolved measurement of the transmission could be made on a single shot basis using a technique developed by David *et al* [8]. In this method a series of diffraction gratings is used to create several

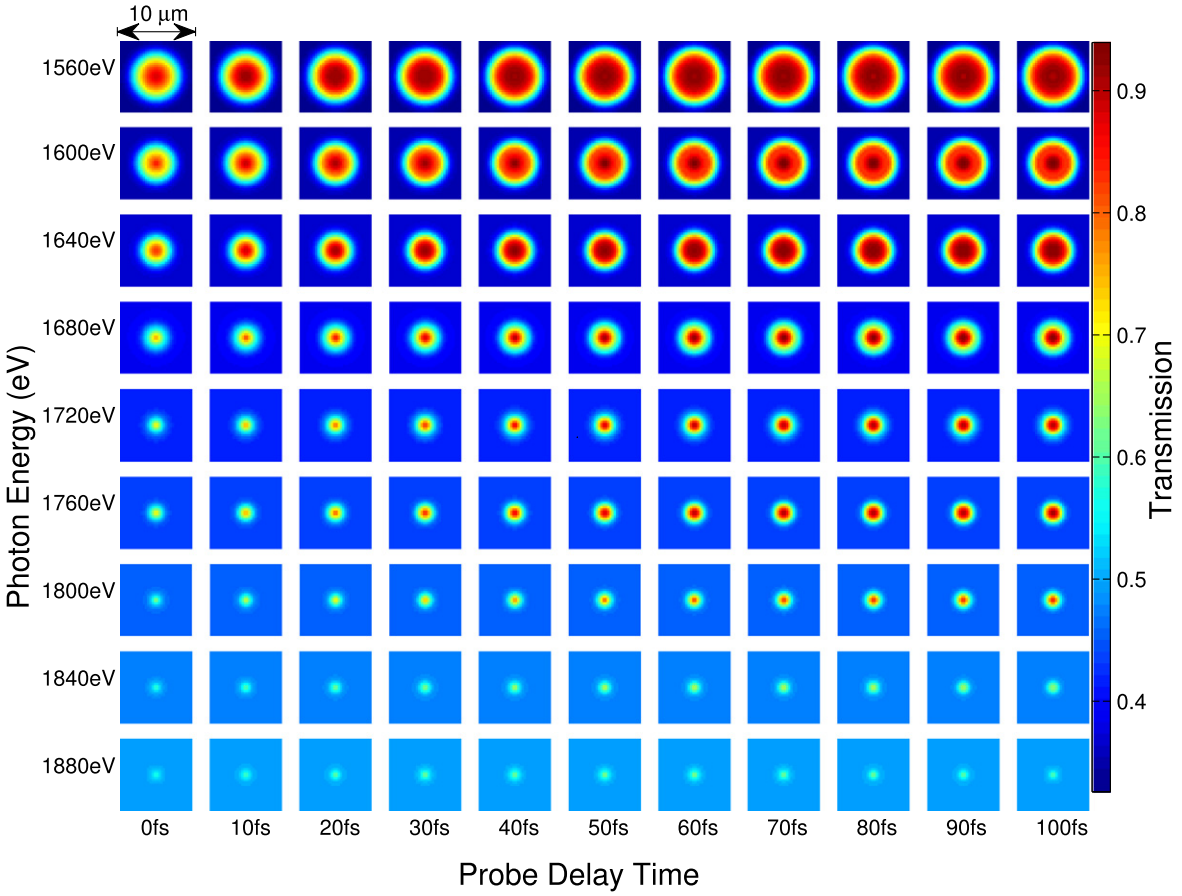

Figure 1. The simulated transmission of probe pulses through an FEL heated 1 μm thick aluminium foil. The delay of the probe pulses with respect to the pump pulse is indicated at the bottom of each column. The photon energy of the pump and probe is shown to the left of the rows.

diffraction orders which scatter at associated angles to the zeroth order main x-ray pulse. The main pulse propagates and is focussed onto the target of interest. A second set of diffraction gratings is placed between the initial gratings and the interaction region, re-scattering the higher order modes such that they too pass through the interaction region, but now with a delay (depending on their order) compared with the zero-order pulse owing to the longer distance they have traversed. Thus within this scheme, a schematic of which can be seen in figure 1 of [8], it is possible to have multiple beams probing the transmission of an FEL-heated plasma from a single FEL pulse. Each of these beams will experience a different time-integrated transmission, as each interacts with a target with a different delay as the charge states within the plasma are evolving. Furthermore, the apparatus can be set up so that the probe beams over-fill the focal spot of the zeroth-order beam. By allowing the probe beams to diverge from their focus before being recorded on a distant detector, such as an x-ray CCD, a spatially resolved (but, for a particular delay, time-integrated) image of the probe beam can be recorded, and by comparing this image with and without a target in place, a spatially resolved recording of the transmitted fraction of the beam can be made. We show below that by studying the differences between such transmission maps for probe beams with different delays, time-resolved information about the charge state evolution can, in principle, be obtained.

2. Simulations

The simulations were performed using the SCFLY collisional-radiative code [6, 7]. The sample simulated was a 1 μm thick aluminium foil oriented normal to the FEL beam. The 1 μm thickness is chosen as it corresponds approximately to one absorption depth just above the *K*-edge of cold aluminium (1560 eV). The SCFLY code generates time dependent opacities and superconfiguration populations given an input FEL radiation field. As the transmission will vary with time and depth in the sample, the simulated sample is divided into ten 100 nm laminae, with the transmitted FEL pulse for one lamina used as the input for the next lamina. The parameters of the FEL were chosen to match approximately those of the experiment in [5]. The spatial distribution used has an effective area of 7 μm^2 with a profile described by a super-Gaussian and the pulse energy is 0.8 mJ (on target). The FEL is tuned to photon energies from 1560 to 1880 eV with a bandwidth of 0.3%. For this work an FEL pulse with a tophat temporal profile of 100 fs duration was used; we will discuss below how this aids the extraction of time-resolved

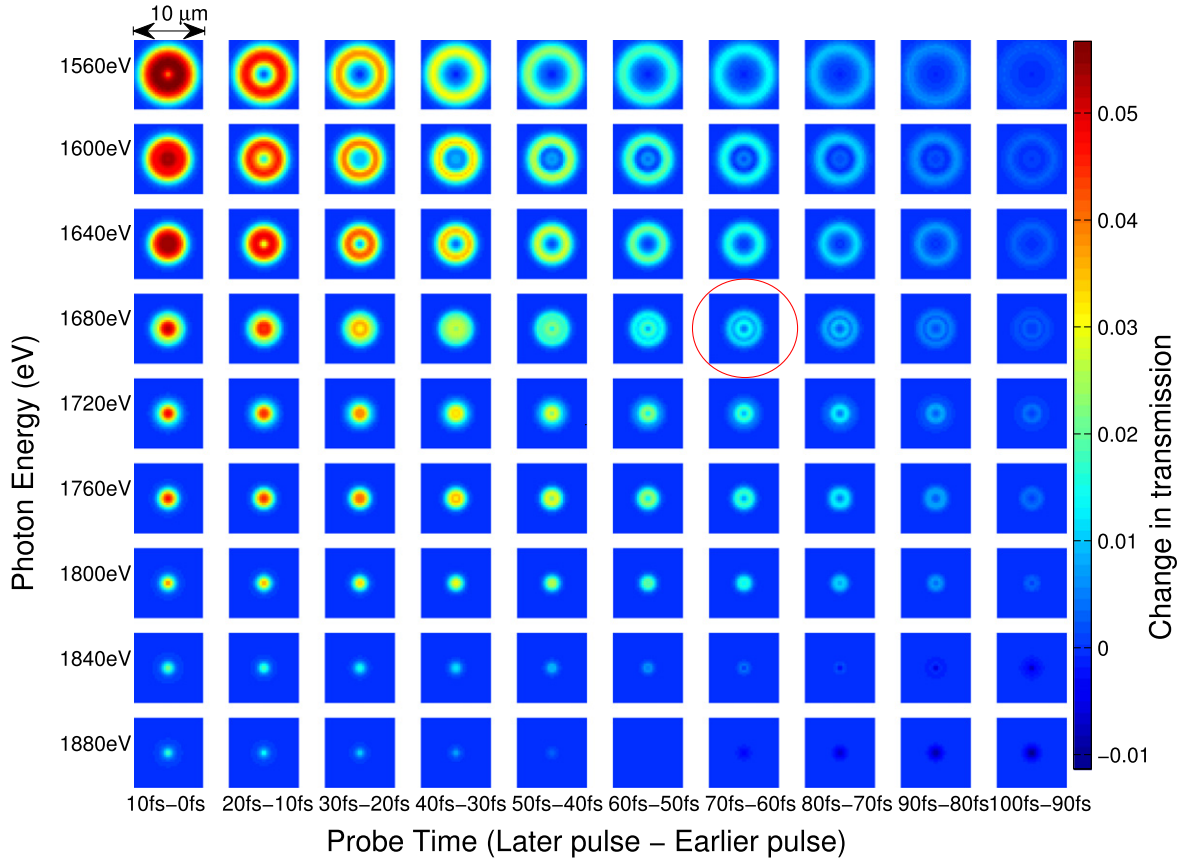

Figure 2. The difference in transmission of two sequential probe pulses, with delays in fsec as indicated at the bottom of each column. The circled example is shown in a larger form in figure 3.

information, but for now note that such a temporal profile is not unrealistic (see figure 2 of the work of Behrens and co-workers [9]). The probe beams are assumed to have the same temporal and spectral structure as the pump FEL pulse, and are assumed to be sufficiently weak that they do not affect the populations and charge states within the sample generated by the main zeroth-order FEL pulse. Hence, the main FEL pulse is used as the only radiation input for the SCFLY simulations. In the simulation the probe beams are propagated through the sample using the attenuation coefficients generated by the simulations. Probe beams with delays between the start of the pump and of the probe ranging from 0 fs to 100 fs in steps of 10 fs were propagated through the simulated heated sample. By dividing the transmitted intensities by the input intensities the transmission of the sample can be derived.

3. Results

Figure 1 shows the transmission of each of the probe beams, with ten different delays, through a 10 μm $\times$ 10 μm square of aluminium, for FEL photon energies ranging from 1560 to 1880 eV. It can be seen that the transmission is greatest at the centre where the pump beam is at its highest intensity. The transmission is generally greater at larger delays between the pump and the probe pulses. This is to be expected, as later in time, as the main pulse is absorbed, more of the atoms within the focal spot are ionised to higher charge states [5]. For a given FEL photon energy there will be a charge state where an ion can no longer absorb a photon through *K*-shell photoionisation, owing to the energy of the *K*-edge of the ion exceeding the photon energy. This reduces the absorption cross-section, increasing the transmission. As the higher charge states are generated later in the pulse the transmission increases over the pulse duration. The transmission of the outer regions, where the FEL intensity is lower, does not change much over the duration of the pulse. There is a change in the transmission of the outer regions as the FEL photon energy is increased, however that is simply due to the cold absorption rate changing. The area of the region which has a different transmission to the cold case decreases with increasing photon energy, due to higher ionisation being required to change the transmission at higher photon energies.

More information can be gleaned by examining the difference between successive probe pulses, i.e. the spatially resolved transmission at time t is subtracted from the image at time $t + 10$ fsec. Given that the probe pulses in this case are tophat, the transmission of the majority of the two pulses will be the same, and will cancel out, with the remainder representing the difference between the transmission at the initial and final 10 fsec the probe pulse. These differences are shown in figure 2.

As would be expected, at the latest times the difference between successive pulses at the centre of the spot is almost

zero, implying that in this region the transmission had reached a steady value at a reasonably early point in the pulse. The outermost region has little change in transmission at any time —also an unsurprising result. Between these two regions the transmission is changing over the duration of the probe pulse. We note that this manifests itself as the appearance of rings in figure 2. Interestingly at a few photon energies there appears to be two rings of larger change in transmission, a point which will be discussed further below. The phenomena in the inner and outermost regions are the simplest to explain. In the central area saturation of the absorption has occurred at a comparatively early time and so later probe pulses will experience the same environment and so have near identical transmission. While in the outermost region the pump pulse is not intense enough to induce saturation of the absorption, hence the transmission of sequential probe pulses is nearly identical.

We return now to the ring structure that is seen in the difference maps at intermediate times. The highlighted example in figure 2 is shown in larger form in figure 3. This image shows the difference in transmission between probe beams which start 60 and 70 fs after the main pump pulse for an FEL photon energy of 1680 eV The double ring structure can clearly be seen. An understanding of the origin of the rings can be obtained by noting that owing to the assumed super-gaussian nature of spatial distribution of the intensity within the focal spot of the x-ray laser, the intensity decreases as a function of radial distance from the centre of the spot, and as a consequence regions at larger radius will, at a specific point in time, be at a lower temperature and lower charge state. As we have already discussed, different charge states have different *K*-edge energies, and the overall transmission is a strong function of the energies of those edges compared with the photon energy of the FEL. Furthermore, recall that what we are plotting is the difference in transmission between two successive temporally top-hat pulses: i.e. we are sensitive to the difference in the opacities between the start and the end of the probe pulses.

In this particular example, with a pump photon energy of 1680 eV, the ring structure is due to spatial and temporal differences in the populations of the 6+ and 7+ ions, as the 7 + ion is the highest charge state with a *K*-edge below 1680 eV (though we note this will depend on the model used for ionisation potential depression (IPD), a matter to which we will return later). Consider the four subfigures in figure 3. These show the opacity of the different radial regions at the central FEL photon energy along with the contributions towards this total of the 6+ and 7+ charge states, taken from the third lamina (i.e. between 200 and 300 nm from the surface upon which the FEL is incident). The arrows on the horizontal axis of the subfigures indicate the start and end points of the probe pulse, and we note that we expect to have a large difference amplitude when the absolute difference in opacity present at these two points of time is large. From the subfigures we see that at the centre of the focal spot the opacity due to both ions is low at the start and end of the probe pulses, and this is due to the high intensity having heated the plasma to such a temperature that both charge states have been burnt through: the difference in intensity is low. A little further out in radius (the top right subfigure) both charge states are present at the start of the probe pulse, with charge state 7+ dominating over that of 6+, and both contribute to the opacity. However, as the plasma heats up later in time, the populations of both reduce, lowering the opacity at the end of the probe pulse compared with that at the start, and thus giving rise to a peak in the difference map.

Moving further out in radius still (bottom left subfigure), we come to another minimum in the difference between the opacity at the start and end of the probe pulses, however here we see that the situation is more complicated. We find that although the total opacity is equal at the start and end of the probe pulse, the contribution to that opacity from the two difference charge states varies enormously—at the start of the probe it is dominated by the 6+ ion, and at the end of the pulse by the 7+ ion. Furthermore, we note that within the simulation there is a large increase in the opacity of the 7+ ion after 70 fsec, between the start and end of the probe pulses. This sudden increase in opacity is directly related to the model being used within the simulations for the IPD, and how it changes as a function of electron density. Within these simulations we have used the Ecker and Kröll (EK) IPD model [10], modified for consistency [11], which is strongly dependent on the electron density. After 70 fsec the plasma has heated sufficiently, and ionised to a degree where suddenly, within this model, the *K*-edge of the 7+ charge state lies lower in energy than the photon energy. Our motivation for using this IPD model is that it has been shown to produce a good fit to experimental data for aluminium by Ciricosta *et al* [2].

Finally, at the largest radius (see the bottom right subfigure figure 3), we are now at such a low FEL intensity that although 6+ ions are produced, the temperature and electron density is sufficiently low that even if any 7+ ions are produced, within the EK IPD model the *K*-edge of this ion stage remains higher in energy than the photon energy, and the opacity is dominated by that of the 6+ ion stage. As the 6+ stage reduces in population during the pulse, as some 7+ is produced, the opacity at the end of the probe pulse is significantly lower than that which exists at the start of the probe pulse, producing a large difference.

As noted above, the subfigures show the simulated history of the opacity at a particular lamina, within which the *K*-edge shifts beyond a set photon energy at a single instant in time. However, this transition occurs earlier in the pulse for higher intensities. The ring patterns in the transmitted intensity are smoothed due to this effect, as when looking at the full transmission through the 1 μm target, each of the ten laminae will experience this transition at a different time owing to the fluence experienced at each depth being reduced by the preceding layers. Some smoothing is also due to the inclusion of the finite bandwidth of the FEL in the simulations.

This smoothing occurs not only spatially in the time-integrated spatial images; no discontinuity is seen in the time-resolved transmission at a particular point in space. To illustrate this, we show in figure 4 the history of the

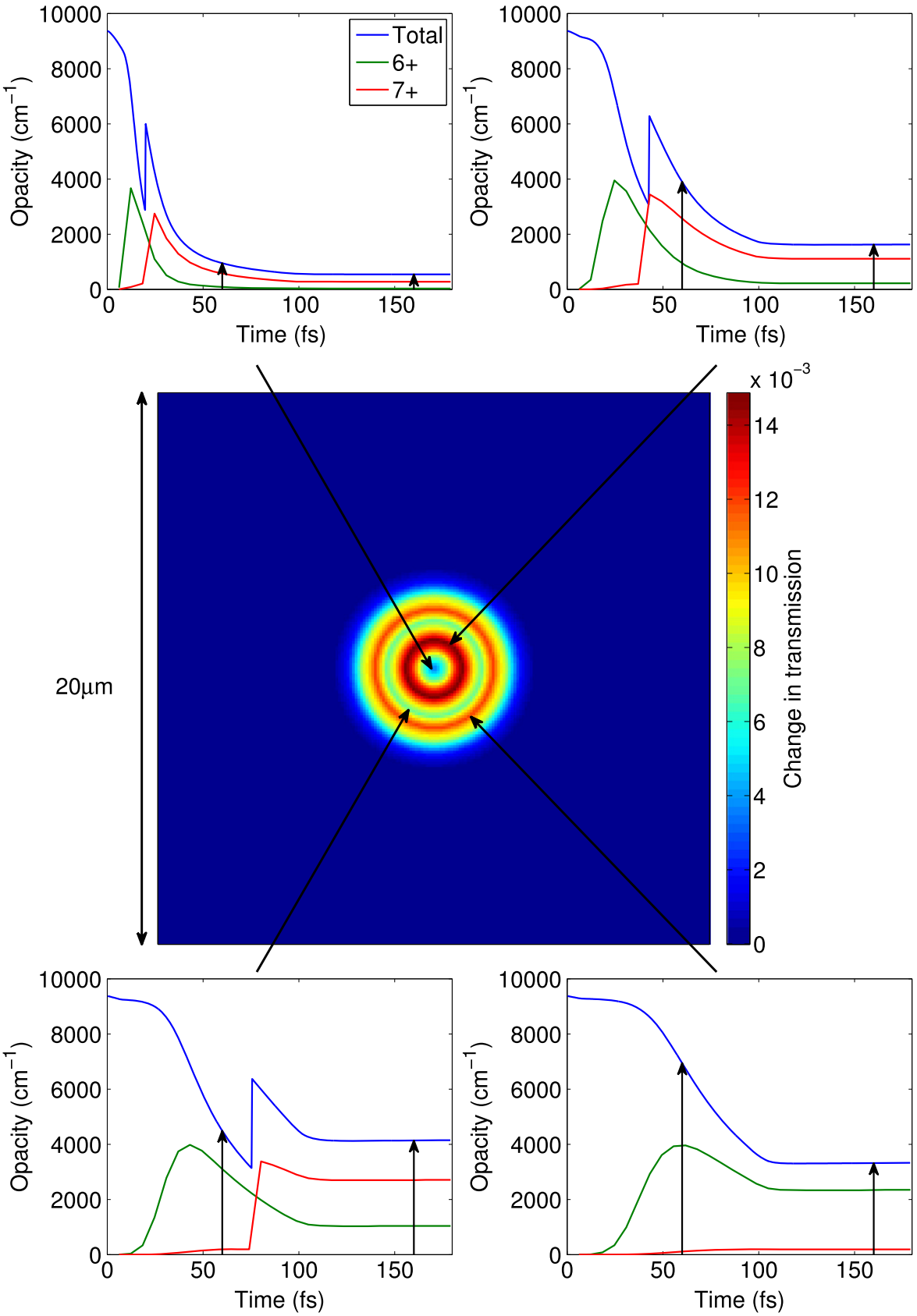

Figure 3. An expanded view of the difference between the transmission of probes delayed by 60 and 70 fs from the pump pulse. The FEL photon energy is tuned to 1680 eV. The subfigures show the simulated total time dependent opacities at 1680 eV, along with contributions towards this total of the 6+ and 7+ charge states, at the spatial regions indicated. The arrows on the subfigures indicate the start and end times of the earlier probe pulse.

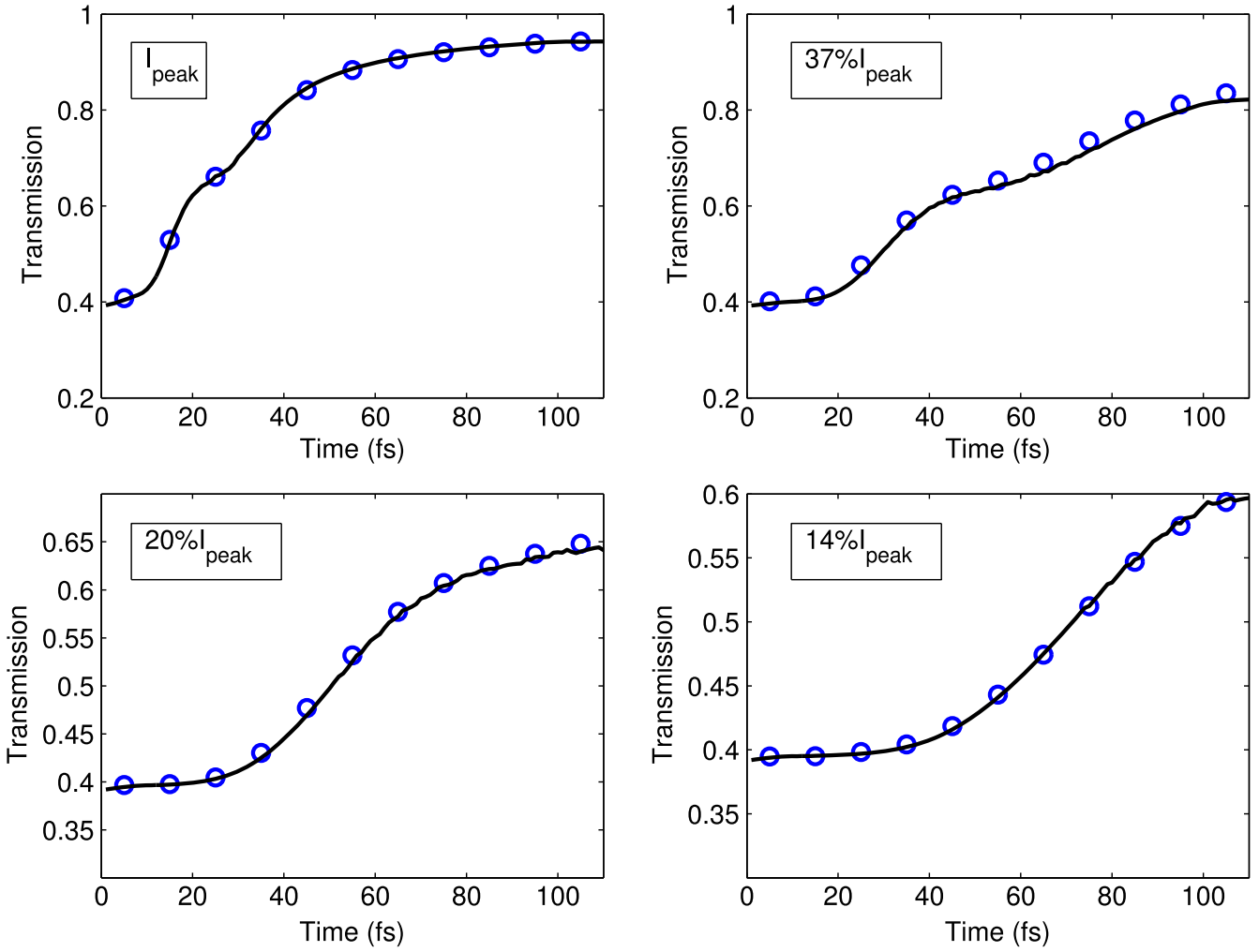

Figure 4. The transmission through the FEL heated aluminium, when pumping with different intensities. the black lines are the values directly from the simulations, while the blue circles are values derived from the differences of transmission of probe pulses. The intensities correspond with those of figure 3.

transmission through the whole sample for four different incident intensities. We see that there is a feature in the full transmission through the sample that occurs at about the time where in the subfigures of figure 3 the *K*-edge of 7+ exceeds the photon energy. However, in the full transmission at a particular intensity this transition is characterised by a reduction in the rate of increase of transmission. This can be attributed to the fact that when the front of the target has transitioned to being highly absorbing, the rear, experiencing a lower intensity, will still have relatively high transmission.

Experimentally one records the time-integrated image, such as that shown in figure 1, but we wish to extract the time-dependent transmission. Using the knowledge of the temporal shape of the FEL pulse it is possible to get the evolution of the transmission of the sample. The final probe pulse has no temporal overlap with the pump pulse, so we assume that the transmission of the final probe beam is the transmission of the sample after the pump pulse. The difference between each probe pulse and the preceding one is then the difference between the transmission of the start of the earlier pulse and the final transmission of the sample. Hence by repeating this process for each of the probe pulses the transmission of the sample can be derived. Figure 4 shows the transmission of the sample at different intensities derived from the total transmission of the probe pulses (blue circles) along with the instantaneous total transmission in the simulations (black lines). These show good agreement with one another indicating this is a possible means of deriving the full evolution of the transmission.

Deriving the full transmission evolution through use of the differences between sequential probe pulses is reliant on the x-ray pulse shape being a tophat. However, an alternative method to extract the temporal profile of the transmission may be possible when the pulse shape is non-tophat. We note that in these simulations the transmission is actually mainly determined by the fluence, rather than the intensity. Thus a possible means of deriving the time-dependence of the transmission, assuming one knows the pulse-shape, would be to examine the transmission of one of the later probe pulses as a function of spatial position, i.e. with different fluences. This would give the transmission as a function of fluence, which would give a time evolution for a given pulse shape.

4. Discussion

The ring structure seen in the difference in transmission images shown above is clearly related to the *K*-edge of a particular charge state changing in time, and moving across the photon energy of the FEL. These features are therefore dependent upon the validity of the IPD model used within the SCFLY atomic kinetics code. The model used in this particular set of simulations is the EK one, which was shown to produce a better fit than the standard Stewart and Pyatt (SP) model [12] for hot-dense Al produced at LCLS, [2]. However, the standard SP model would have still produced similar structures, albeit at different FEL wavelengths, due to both models predicting a change in the degree of IPD in time, as the electron density increases (the IPD for both SP and EK scales as $n^{1/3}$).

The technique described by the simulations would appear to show the region over which the *K*-edge shifts such that an ionic species can absorb the FEL radiation. That is to say, the technique is sensitive to the time evolution of the density of states of the conduction band for particular ion stages. Such measurements could then lend themselves to the validation of simple IPD models (like SP or EK), as well as of more elaborate calculations based on DFT [13]. Furthering of our understanding of these systems is of fundamental interest, and we posit that the sorts of transmission experiments that we have simulated here may be able to provide important information on both the time-evolution of the charge states within the plasma, as well as providing an alternate, complementary, method to emission spectroscopy as a means of studying density effects in these hot, dense plasmas.

5. Conclusions

In conclusion we have shown that by using a split and delay setup it is feasible to follow the evolution of the transmission of an FEL heated aluminium sample on a femtosecond timescale by recording delayed space-resolved transmission images. It is interesting to note that the form of the IPD could have a profound effect on the observed changes in transmission at certain photon energies, and hence such simple time-integrated, yet delayed, transmission experiments could, in principle, yield interesting information about the evolution of the charge states and their *K*-edges within an x-ray heated plasma.

Acknowledgments

The authors would like to thank Christian David and Mikako Makita from PSI, Switzerland, for useful discussions. DSR, OC and JSW are grateful to the UK EPSRC for funding under grant number EP/H035877/1. SMV gratefully acknowledges funding from The Royal Society.

References

[1] Vinko S M *et al* 2012 *Nature* **482** 59–62
[2] Ciricosta O *et al* 2012 *Phys. Rev. Lett.* **109** 065002
[3] Cho B I *et al* 2012 *Phys. Rev. Lett.* **109** 245003
[4] Rackstraw D *et al* 2014 *High Energy Density Phys.* **11** 59–69
[5] Rackstraw D S *et al* 2015 *Phys. Rev. Lett.* **114** 015003
[6] Chung H K, Chen M H and Lee R W 2007 *High Energy Density Phys.* **3** 57–64
[7] Ciricosta O, Chung H K, Lee R W and Wark J S 2011 *High Energy Density Phys.* **7** 111–6
[8] David C *et al* 2015 *Sci. Rep.* **5** 7644
[9] Behrens C *et al* 2014 *Nat. Commun.* **5** 3762
[10] Ecker G and Kröll W 1963 *Phys. Fluids* **6** 62
[11] Preston T R, Vinko S M, Ciricosta O, Chung H K, Lee R W and Wark J S 2013 *High Energy Density Phys.* **9** 258–63
[12] Stewart J C and Pyatt K D 1966 *Astrophys. J.* **144** 1203
[13] Vinko S, Ciricosta O and Wark J 2014 *Nat. Commun.* **5** 3533